

*Article*

## The Empirical Formula for the Stiffness of a Spur Gear Pair Based on Finite Element Solutions

Thiwa Nantapak<sup>a</sup>, Kornsara Srisarakorn<sup>b</sup>, Thanakorn Tantipiriyapongs<sup>c</sup>,  
Nitchawat Deecharoen<sup>d</sup>, and Chanat Ratanasumawong<sup>e,\*</sup>

Department of Mechanical Engineering, Faculty of Engineering, Chulalongkorn University, Bangkok, Thailand

E-mail: <sup>a</sup>Thiwa.N@Chula.ac.th, <sup>b</sup>Kornsarasrisarakorn@gmail.com, <sup>c</sup>tanti.thanakorn@gmail.com, <sup>d</sup>nitchawat.dee@gmail.com, <sup>e,\*</sup>Chanat.r@chula.ac.th (Corresponding author)

**Abstract.** Gear meshing stiffness is commonly determined by the analytical method or the finite element method (FEM). Both methods can be used to determine the meshing stiffness but the calculation for the analytical method is more complicated, while the FEM is impacted by the tooth contact setting and large computation time. Thus, both methods have limitations for practical use. Here, an empirical formula was proposed to calculate meshing stiffness of a spur gear pair with gear ratio 1:1 in moderate to large load conditions. The formula was divided into two parts as 1) an equation used to calculate the stiffness of the gear cylinder derived from the elasticity equations, and 2) an empirical formula to determine the meshing stiffness of the tooth pair based on FEM solutions. The second part of the formula was constructed by selecting the related parameters, finding the appropriate formula pattern, and determining the relation between these parameters and tooth stiffness at any meshing position. Meshing stiffness of the gear pair was determined by combining the stiffness of two parts connected in series. Accuracy of the empirical formula was verified by comparing the calculated meshing stiffness with previous research and indicated that the calculated meshing stiffness conformed well with other studies. Our proposed empirical formula can be applied to any spur gear pair with gear ratio 1:1 to accurately determine gear meshing stiffness.

**Keywords:** Tooth stiffness, spur gear, empirical formula, finite element method.

ENGINEERING JOURNAL Volume 26 Issue 1

Received 4 January 2021

Accepted 23 December 2021

Published 31 January 2022

Online at <https://engj.org/>

DOI:10.4186/ej.2022.26.1.11

## 1. Introduction

The meshing stiffness of a spur gear pair is an important parameter that is used to study gear dynamics and vibration. If known, meshing stiffness can be used in a vibration model to accurately predict gear vibration characteristics. Methods used to study gear meshing stiffness can be classified into the analytical method [1-12], the finite element method (FEM) [13-19], experimental methods [20-21], and methods that combine analytical method and FEM [22-25].

For the analytical method, a gear tooth is normally modeled as a cantilever beam fixed at its base circle or root circle. The meshing stiffness of the gear pair is calculated from the bending stiffness and the Hertzian contact stiffness. Some researchers attempted to improve the accuracy of their methods by including the effect of shear stiffness, axial stiffness, and stiffness of the fillet-foundation in the calculations. The stiffness of each part was frequently calculated based on the theory of elasticity [1, 3-4] or the energy method [2, 6-12]. Advantages of the analytical method are that it can be applied to the gear pair easier than the other methods, and can be modified to include the effects of gear modifications, cracks, or other gear defects in the calculations [4-11]. However, methods to derive the equations and the calculation of the necessary parameters are complicated and require computer simulation.

Besides the analytical method, FEM is also a powerful method to determine the stiffness of gear teeth. Since the model used in the FEM was constructed to match with the actual gear pair, the result from FEM was more accurate compared to the analytical method. However, the FEM also has problems resolving the tooth contact settings in the modeling stage, and requires large computation time. This is because the gear contact problem is non-linear and requires a small mesh element size near the contact point and also an iterative calculation. To solve this problem, some researchers used the linear FEM for the tooth deflection and the Hertzian contact theory at the contact area [22, 25]. This reduced the computational effort compared to the conventional FEM. Another important disadvantage of the FEM method is that the result of a specific gear pair cannot be applied to other gear pairs having different parameters. The calculation must be performed for each new gear pair. This makes the FEM unsuitable for practical use.

For the reasons stated above, a formula that relates directly to gear parameters and can be easily applied in practice is required. Here, we propose a method to construct an empirical formula to calculate spur gear meshing stiffness for the gear ratio 1:1 in moderate to large load conditions. The formula is divided into two parts as an equation to calculate the stiffness of the gear body that is derived based on elasticity equations, and an empirical equation of tooth meshing stiffness that is constructed based on FE solutions. We verified our proposed empirical formula against the gear meshing stiffness results reported by previous researchers.

## 2. Meshing Stiffness of a Spur Gear Pair

The meshing stiffness of a spur gear pair is attributed to the deformation of many gear parts that include the cylindrical body, gear tooth bending and contact area as shown in Fig. 1. Total gear meshing stiffness ( $k$ ) can be calculated by connecting the stiffness of each part in series as shown by equation

$$\frac{1}{k} = \frac{1}{k_{C,1}} + \frac{1}{k_{b,1}} + \frac{1}{k_{h,1}} + \frac{1}{k_{h,2}} + \frac{1}{k_{b,2}} + \frac{1}{k_{C,2}} \quad (1).$$

The subscript “C” means the cylindrical body, “b” means the gear tooth bending, “h” means the tooth contact, “1” and “2” means the driving side and the driven side. Although the contact stiffness ( $k_h$ ) is affected by the material properties and geometries of both driving and driven gears, it can be divided to the individual tooth as the apparent contact stiffness  $k_{h,1}$  and  $k_{h,2}$ . This consideration is suited to the finite element solution that the calculated displacement at the contact point of each gear already includes the deformation of the whole part including the tooth contact. To simplify the calculation, we considered the stiffness attributed to gear tooth bending and gear tooth contact area together. Hence the gear stiffness model used in this paper is composed of the stiffness of the cylindrical body of the driving and driven gear and the meshing stiffness of the driving and driven gear tooth as shown by equations

$$\frac{1}{k} = \frac{1}{k_1} + \frac{1}{k_2} = \frac{1}{k_{C,1}} + \frac{1}{k_T} + \frac{1}{k_{C,2}} \quad (2),$$

and

$$\frac{1}{k_T} = \frac{1}{k_{T,1}} + \frac{1}{k_{T,2}} = \left( \frac{1}{k_{b,1}} + \frac{1}{k_{h,1}} \right) + \left( \frac{1}{k_{b,2}} + \frac{1}{k_{h,2}} \right) \quad (3),$$

where the subscript “T” means the gear tooth.

For single tooth pair meshing,  $k_T$  is the stiffness of only one tooth pair and can be calculated directly from Eq. (3). However, for double teeth meshing,  $k_T$  is calculated by connecting the stiffness of each tooth pair meshing at the same time in parallel as shown by equation

$$k_T = (k_T)_{1st} + (k_T)_{2nd} \quad (4),$$

where the subscripts “1st” and “2nd” mean the first and the second meshing pair, respectively.

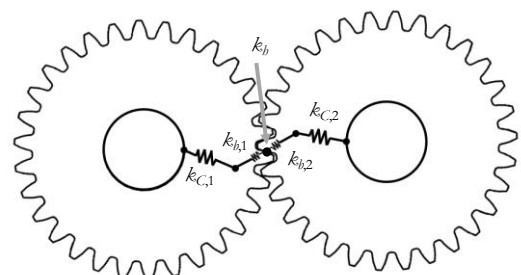


Fig. 1. Meshing stiffness of a spur gear pair.

To calculate the gear meshing stiffness, the stiffness of the cylindrical part and the stiffness of the gear tooth are considered separately. The shape of the cylindrical body is much simpler than the shape of the gear tooth and can be determined analytically. Moreover, the shape of the cylindrical body can be designed with various hub or hole sizes, even if the tooth parameters are fixed. Therefore, the method to determine the cylindrical part and the gear tooth separately can be applied to any gear pair having the same tooth parameters but different cylindrical shape. On the other hand, the geometry of the gear tooth is much more complicated than the cylindrical body. Determining the meshing stiffness of this part analytically requires complicated calculations that are not suitable in practice. Thus, an empirical formula for determining the meshing stiffness of the gear tooth is required. Here, we constructed this empirical formula based on data from the finite element analysis.

### 3. Stiffness of The Cylindrical Body

The gear cylindrical body was modeled as a simple hollow cylinder. The cylinder is fixed at the inner surface and moment is applied at the outer surface. The equation for calculating the stiffness of this part can be derived based on the basic stress-strain-displacement equations in cylindrical coordinates. The stress function of this problem was shown in Ref. [26]. By substituting the stress function into the stress equation and using the stress-strain relation and strain-displacement equation with the boundary condition that the displacement at the fixed surface equals to zero, the displacement in radial direction  $u$  and circumferential direction  $v$  can be determined. The deformation in this case will occur only in the circumferential direction. There is no deformation in the radial direction. The stiffness of the cylindrical body can be calculated by

$$k_c = \frac{4G\pi r_i^2 b}{r^2 - r_i^2} \quad (5),$$

where  $r_i$  is the radius of the inner cylinder,  $r$  is the radius at the cylinder where the displacement  $v$  is calculated,  $b$  is the width of the cylinder and  $G$  is the shear modulus.

To verify the accuracy of Eq. (5), the calculated results were compared to the finite element solutions as shown in

Table 1. From the table, the stiffness of a smaller cylinder is higher than a larger cylinder. Stiffness results calculated from the analytical equation were very close to those calculated from the finite element method, with maximum error less than 0.5%. Thus, Eq. (5) is very accurate to use for calculating the stiffness of the cylindrical body.

## 4. Effects of Loads and Gear Parameters on Tooth Meshing Stiffness

### 4.1. Gears Used for Investigation

To construct the empirical formula for calculating the gear tooth meshing stiffness, it is necessary to know the effects of gear parameters. Parameters that may affect gear tooth meshing stiffness are module, pressure angle, number of teeth, face width, modulus of elasticity, magnitude of applied force, and meshing position. Table 2 shows different gear sets with various parameters. The gear considered in this paper was the standard gear that was conjugate with the standard basic rack profile in ISO 53 without any modification. The gears with pressure angle  $14.5^\circ$  and  $25^\circ$  that are widely used were also included in this study. Meshing stiffness of these gear sets was calculated by the finite element method (FEM) and results were used as the database for constructing the empirical formula.

From Table 2, gears A, B, C and D have modules 2, 3, 4 and 5 mm, respectively while the other parameters are identical. These were used to study the effect of gear module and the effect of force applied along the line of action. The effect of the number of teeth was determined by comparing gears A, E and F that have numbers of teeth at 30, 45 and 60. The effect of pressure angle was known from the results of gears A, G and H and gears C, I and J.

### 4.2. Finite Element Calculation

Finite element analysis in this study was performed using the ANSYS program. Since the contact problem was non-linear, the required calculation time was considerably more than for a normal linear problem and some assumptions were necessary to simplify the calculation. These assumptions were 1. Force is distributed uniformly along the face width direction hence the problem can be

Table 1. Stiffness of the cylindrical body calculated from the analytical method and FEM.

Model	Shear modulus, $G$ (GPa)	Inner radius, $r_i$ (mm)	Outer radius, $r$ (mm)	Width, $b$ (mm)	Stiffness Anal. cal. (MN/m)	Stiffness FEM (MN/m)	Error %
A	76.92	15	27.55	20	8146.51	8149.00	0.03
B	76.92	15	41.35	20	2929.71	2931.14	0.05
C	76.92	15	55.15	20	1544.47	1548.97	0.29
D	76.92	15	68.95	20	960.46	965.24	0.50
E	76.92	15	42.55	20	2743.66	2745.98	0.08
F	76.92	15	57.55	20	1409.14	1409.19	0.01

Table 2. Gear parameters.

Parameter			Model									
			A	B	C	D	E	F	G	H	I	J
Tooth number	$\zeta$		30	30	30	30	45	60	30	30	30	30
Module	$m$	mm	2	3	4	5	2	2	2	2	4	4
Pressure angle	$\alpha$	deg	20	20	20	20	20	20	14.5	25	14.5	25
Face width	$b$	mm					20					
Gear ratio							1:1					
Shaft diameter		mm					30					
Young's modulus	$E$	GPa					200					
Poisson's ratio	$\nu$						0.3					
Applied force	$F$	N	2364.8,	3547.3,	4729.7,	5912,	5912	5912	5912	5912	5912	5912
				7094.6								

considered to be a two-dimensional plane strain, 2. Sliding friction is neglected in the calculation, 3. The gear rotates at low velocity, therefore a quasi-static condition is assumed.

The calculation procedure is briefly described as follows. First, the spur gear model was drawn by a computer aided design (CAD) program, and then the spur gear pair was set to mesh at a specific position. The line of action was set to align along the vertical direction as shown in Fig. 2(a), hence deformation along the line of action used to calculate gear stiffness can be simply read from displacement in the  $y$ -direction. The type of contact between driving and driven gear was set as frictionless. This allows the contact surfaces to slide but they cannot overlap.

The element type was set to be all triangles. Sizes of elements varied depending on their positions. Element size at the contact area was about  $5 \mu\text{m}$  and small enough compared with the size of the gear tooth as shown in Fig. 2(b). The boundary condition at the hole of the driving gear was set to be frictionless support, while the support at the driven side was set as fixed support. The distributed force corresponding to applied torque was applied at the keyway of the driving gear.

When the calculation was completed, the pattern of stress distribution and the surface displacement on the gear teeth was checked. Around the contact area, the driven surface curvature was smooth, and the maximum displacement value in the  $y$ -direction occurred at the point crossing the line of action. The displacement at this point was measured, and the meshing stiffness of the driven gear was calculated from

$$k_2 = \frac{F}{\delta} \quad (6),$$

where  $F$  is the equivalent force applied along the line of action and  $\delta$  is the displacement at the measured point of the driven tooth. It should be noted that  $k_2$  in Eq. (6) is the stiffness attributed to the deformation of both cylindrical body and driven gear tooth. The stiffness at the other meshing positions was determined by setting the

new meshing position and then following the same calculation method.

The graph of the stiffness  $k_2$  of the driven gear at various meshing positions is shown in Fig. 3. For the gear ratio 1:1 focused here, the stiffness of the driving gear at the same position on the gear tooth must be equal to the stiffness of the driven gear, hence the stiffness  $k_1$  was plotted as the duplicate of the stiffness  $k_2$  with mirror symmetry around the pitch point. The stiffness of the gear pair  $k$  can be calculated by connecting the stiffness of the driving and driven gears in series as shown in Eq. (2).

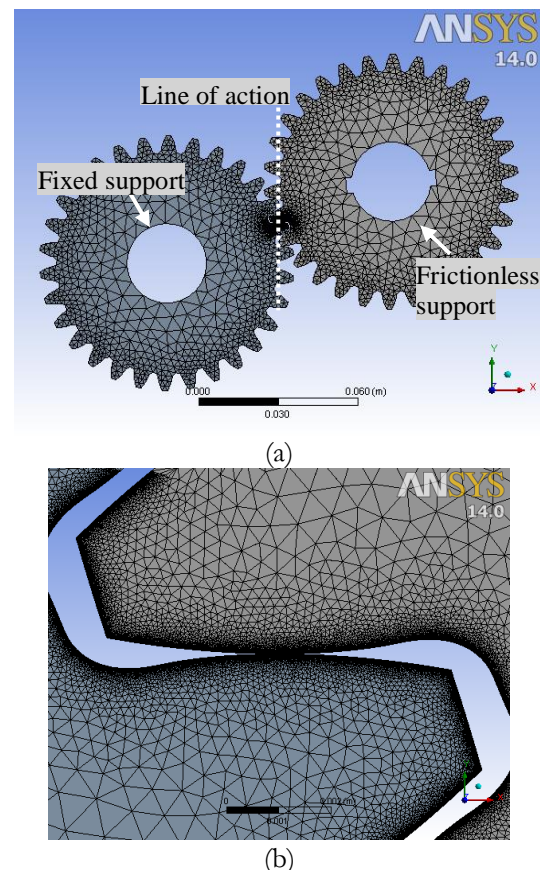


Fig. 2. Gear model and boundary condition for FEM calculation.

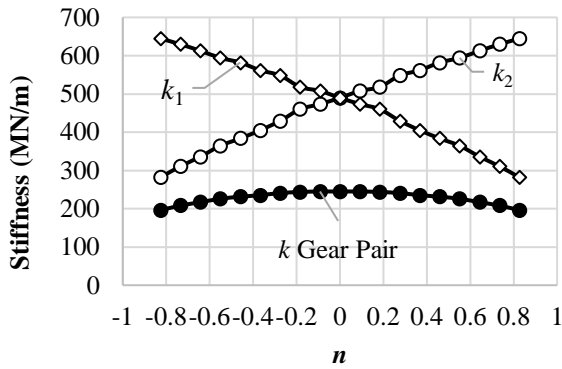


Fig. 3. Meshing stiffness of driving gear, driven gear and total stiffness of a gear pair.

In Fig. 3, meshing position  $n$  is a dimensionless parameter calculated from the distance along the line of action measured from the pitch point to the contact point divided by the base pitch. The parameter  $n$  is used instead of the distance from the pitch point or the rotating angle because the parameter  $n$  of any gear pair is almost the same, even for gear pairs that have different parameters, tooth size, or shape. On the other hand, if the distance from the pitch point or rotating angle is used, these values change when the gear parameters are varied, making it more difficult to compare the results obtained from gear pairs with different parameters.

The ranges of  $n$  are from -1 to 1;  $n$  is equal to zero at the pitch point and has a negative value at the meshing position before the pitch point. The position of  $n$  close to

-1 represents the position close to the point where meshing starts and the tooth root of the driving gear meshes with the tooth tip of the driven gear. After the pitch point,  $n$  becomes a positive value. Meshing will finish when  $n$  is close to 1 as the position where the tooth tip of driving gear meshes with the tooth root of the driven gear. Since the tooth root is thicker than the tooth tip, the stiffness at this portion is larger than the stiffness at the tooth tip.

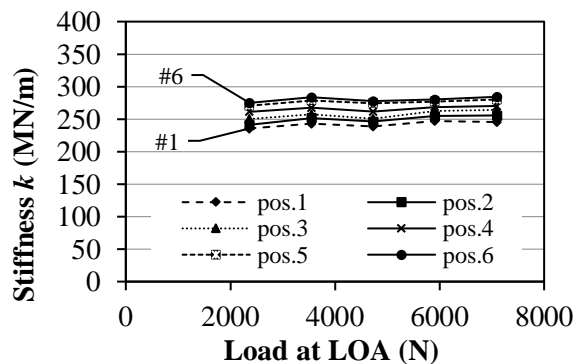
The stiffness of only gear tooth or only meshing part can be calculated by subtracting the stiffness of the cylinder part from the overall stiffness by using Eqs. (2) and (5).

### 4.3. FEM Results

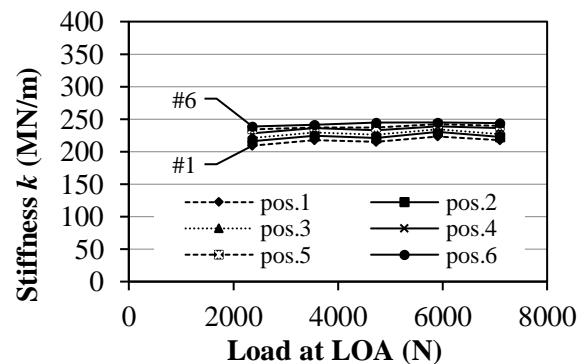
#### 4.3.1. Meshing stiffness of the gear pair subjected to various loads

The contact of gear pairs is a non-linear problem, hence the effect of the applied load on the stiffness also required investigation. The effect of applied load on meshing stiffness is shown in Fig. 4. In Fig. 4, the stiffness of the gear pairs A, B, C and D at some meshing positions were plotted against load. Numbers in the graph represent the position along the meshing position from the point where meshing starts (#1) to the pitch point (#6).

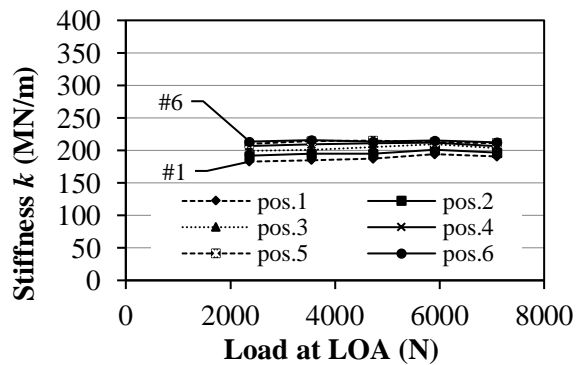
Since moderate and large loads were used in the calculation here, stiffness was almost unchanged with load. These results agree with ISO 6336-1 [27] that implies the



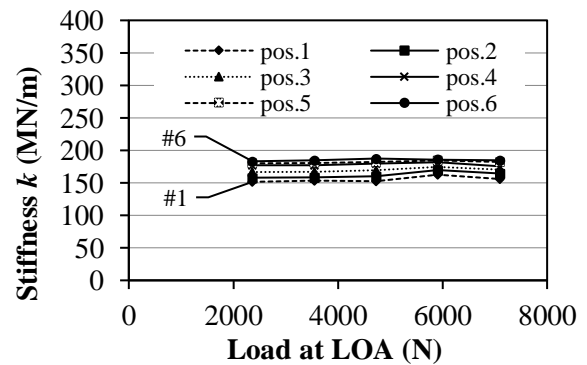
(a) Gear A (module 2 mm)



(b) Gear B (module 3 mm)



(c) Gear C (module 4 mm)



(d) Gear D (module 5 mm)

Fig. 4. Meshing stiffness of gear pairs subjected to various loads.

stiffness does not change with load when applied load is large enough, and the method to determine the tooth stiffness in ISO 6336-1 can be applied when the specific loading (load per face width) is more than 100 N/mm. For the results in Fig. 4, the specific loads in all cases were more than 118 N/mm that were slightly larger than the value 100 N/mm in ISO 6336-1.

For the other gear pairs in Table 2, since the specific loads were larger than 118 N/mm, it is expected that the stiffness is almost unchanged with load. Hence the empirical formula that will be described further can be considered to be applicable when the specific load is larger than 118 N/mm.

#### 4.3.2. Effect of gear parameters

Results obtained from the FEM reveal the effects of gear parameters on gear and tooth stiffness. Figures 5-7 show the effect of module, number of teeth and pressure angle, respectively. In these figures, subfigures (a) are the stiffness of the driven gear calculated from Eq. (6). By connecting the stiffness of the driving gear to the stiffness of the driven gear, the stiffness of the gear pair is obtained as shown in subfigures (c). If the stiffness of the cylinder part is subtracted from the stiffness of the driven gear in subfigures (a), the stiffness of only the driven tooth is obtained in subfigures (b). In the same way, the stiffness of only the tooth pair part is known by connecting the stiffness of the driving and driven tooth in series, or by subtracting the stiffness of the cylinder part from the stiffness of the gear pair in subfigures (c). The stiffness of the tooth pair part is shown in subfigures (d).

##### 4.3.2.1. Effect of module

In Fig. 5(a) and (c), the gear having a smaller module had greater stiffness than the gear having a larger module. The slopes of the stiffness line in Fig. 5(a) increased when the module decreased. The shapes of the stiffness curve of the gear pair in Fig. 5(c) tended to be slightly flatter for the larger module gear. Differences in slope and magnitude of stiffness were smaller when the module became larger.

On the other hand, when considering only the gear tooth in Fig. 5(b) and (d), tooth stiffness was larger than the gear stiffness. The module does not affect gear tooth stiffness as expected. Since varying modules without changing any other parameters will affect only the size of the gear tooth, but the shape of the tooth profile remains the same. Based on the similarity in mechanics, the stiffness should be unchanged. These results also confirm the correctness of the calculation. Thus, the difference in gear stiffness resulted from the cylindrical body part, or in other words, the stiffness of the cylindrical part significantly affected the stiffness of the whole gear. The effect of the cylindrical body on the gear stiffness agrees well with the results reported in the refs. [15] and [22].

##### 4.3.2.2. Effect of number of teeth

The effect of number of teeth on stiffness is shown in Fig. 6. Results in Fig. 6(a) and (c) show that gears having fewer teeth had higher stiffness than gears with more teeth. The slopes of the stiffness graphs in Fig. 6(a) changed

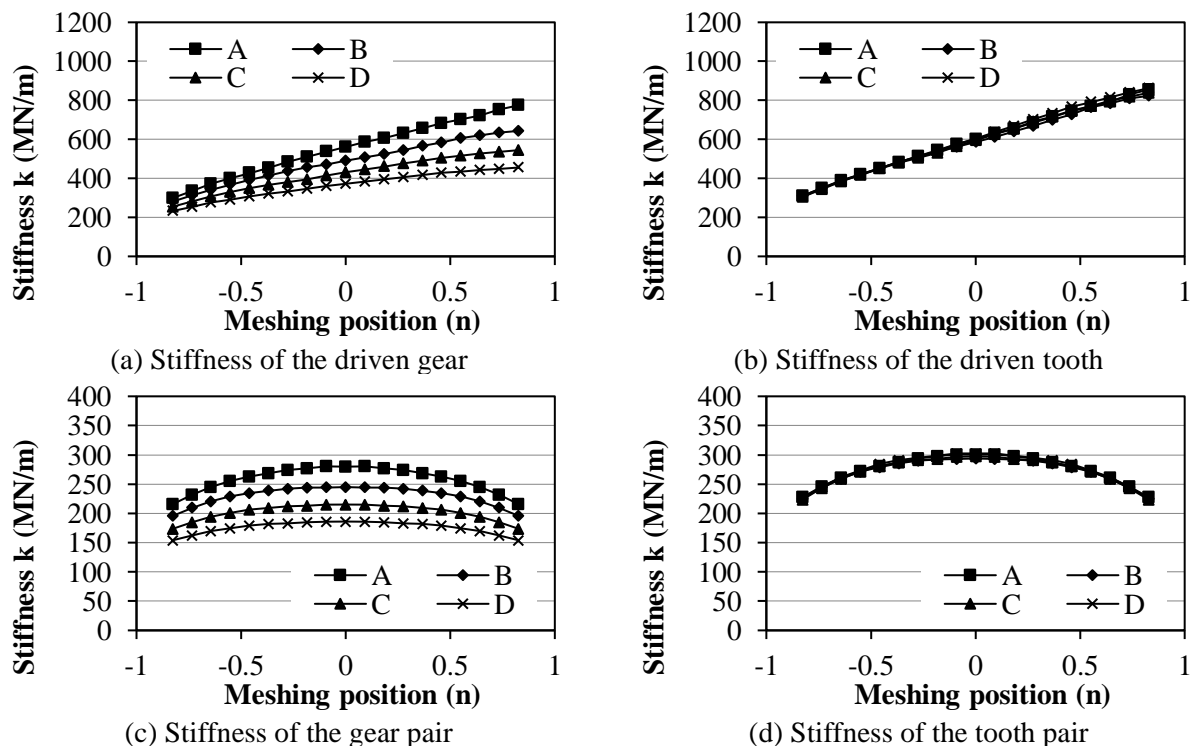


Fig. 5. Effect of module on meshing stiffness.

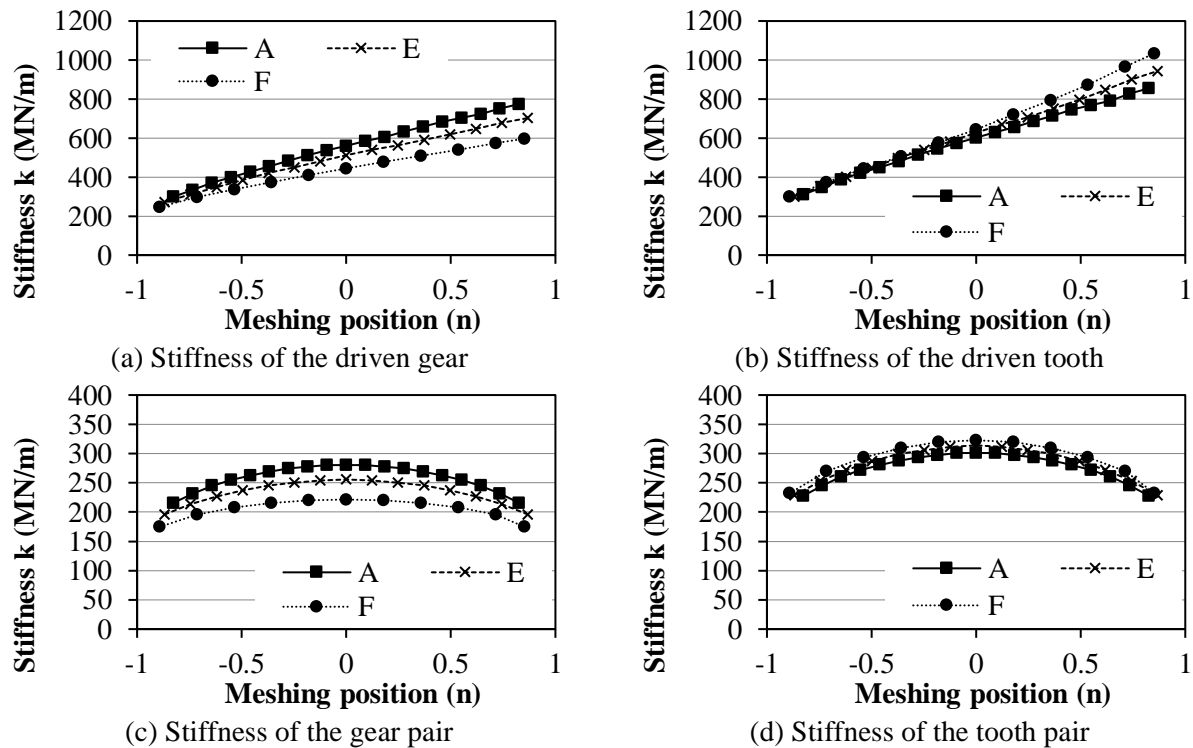


Fig. 6. Effect of number of teeth on meshing stiffness.

when the number of teeth varied. The tooth stiffness of these gears are shown in Fig. 6(b) and (d). In contrast to gear stiffness, the tooth stiffness of gear having fewer teeth was lower than gears with more teeth. Since the ratio between the diameter of the root circle and the base circle varies with number of teeth, and affects the shape of gear tooth, the tooth root portion of the gear having more teeth is thicker than the gear with fewer teeth. This affected the stiffness at the tooth root in Fig. 6(b) of the gear with more teeth to be higher than the gear with fewer teeth. However, the shapes of stiffness curves of the tooth pair in Fig. 6(d) were similar. The amounts of stiffness in Fig. 6(b) and (d) were close together comparing with those in Fig. 6(a) and (b). This indicates that the stiffness of the cylindrical body part also significantly affects the stiffness of the whole gear.

#### 4.3.2.3. Effect of pressure angle

Figure 7 shows the stiffness of gears having different pressure angles. The gear sets G-A-H (square mark) and I-C-J (triangle mark) have pressure angle  $14.5^\circ$ ,  $20^\circ$  and  $25^\circ$ , respectively, but the gears G, A and H have module 2 mm, whereas the gears I, C and J have module 4 mm. When considering only the tooth stiffness in Fig. 7(b) and (d), it is obvious that the module did not affect the gear tooth stiffness. The stiffness of the gear set G-A-H almost completely identical with the gear set I-C-J. The stiffness of gear with pressure angle of  $25^\circ$  (grey mark) was larger than gear with pressure angle of  $20^\circ$  (black mark) and gear with pressure angle of  $14.5^\circ$  (white mark), respectively. Differences in meshing stiffness at the tooth root and

tooth tip, shown by the slope of the lines in Fig. 7(b), were larger when the pressure angle increased. This result agreed with the shape of gear teeth. The difference between the thickness at the tooth root and tooth tip of gears having a higher pressure angle was larger than for gears having a smaller pressure angle. For this reason, in Fig. 7(d), the stiffness of the gear pair with larger pressure angle had more convex shape than the gear pair with smaller pressure angle.

## 5. Empirical Formula for Gear Tooth Meshing Stiffness

### 5.1. Form of the Empirical Formula

In the previous section, the effects of gear parameters on tooth meshing stiffness were already known. However, to construct an empirical formula to calculate tooth meshing stiffness, it is necessary to know which parameters should be added into the formula, and the relation among these parameters. By comparing a spur gear tooth with a rectangular cross section cantilever beam, it is expected that the gear tooth meshing stiffness at a specific meshing position will be the product of the modulus of elasticity  $E$ , face width  $b$ , and also the ratio of tooth thickness at the contact point  $s$  and the length from the tooth root to the contact point  $L$ . However, at a specific point, the ratio  $s/L$  is constant for the standard gears having the same pressure angle and teeth number regardless of the size of gear tooth or module. This is also supported by the results in the section 4 that the module does not affect the tooth stiffness.

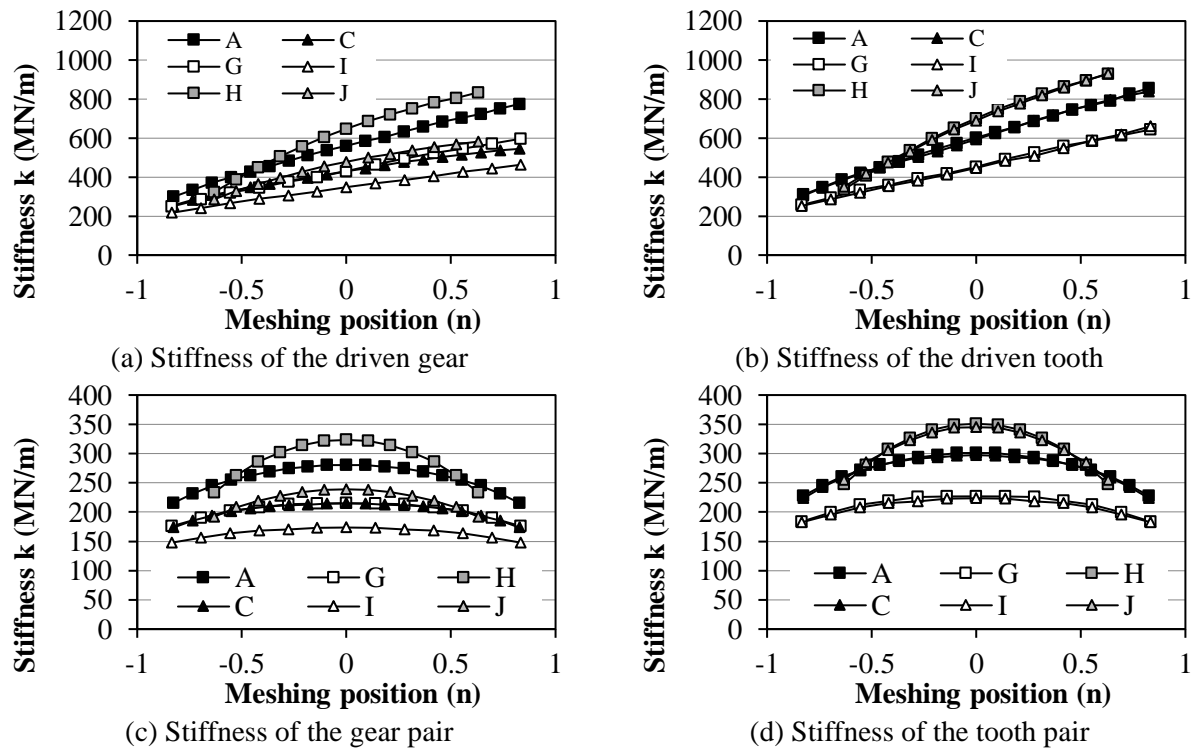


Fig. 7. Effect of pressure angle on meshing stiffness.

At different meshing positions, the ratio  $s/L$  changes, hence tooth stiffness is a function of meshing position  $n$ . From the result of the driven tooth in Figs. 5-7(b), tooth stiffness had a linear relation with the meshing position  $n$ , hence the empirical formula can be written in the form

$$k_{T,2} = Eb(An + B) \quad (7),$$

where  $A$  and  $B$  are constants.

The stiffness of the driving tooth and the driven tooth at the same position on the gear tooth must be equal; however, at a specific meshing position, the contact positions on the driving tooth and driven tooth are different but mirror-symmetrical around the pitch point. Therefore, the value of  $n$  in Eq. (7) must be substituted by  $-n$  for the driving tooth stiffness. The meshing stiffness of the driving tooth is

$$k_{T,1} = Eb(-An + B) \quad (8).$$

The stiffness of the tooth pair can be calculated by connecting the driving and driven tooth meshing stiffness in series, hence the stiffness of the tooth pair is

$$k_T = \frac{Eb}{2B} [B^2 - (An)^2] \quad (9).$$

It is known from Eq. (9) that the stiffness of the tooth pair can be approximated as a quadratic function. The ratio  $s/L$  will change for gears having different number of teeth and pressure angles. Therefore, for these gears, the corrections were added into the formula. The number of teeth affects the amount of the stiffness. On the other hand, the pressure angle affects both amount of the stiffness and the shape of stiffness curve. Since only the pressure angles of  $14.5^\circ$ ,  $20^\circ$ , and  $25^\circ$  are widely used, the pressure angle correction of each pressure angle was used

specifically, and was designed to be the function of meshing position  $n$ . From Eq. (9) and the above description, the empirical formula used to calculate the meshing stiffness of the tooth pair can be written in the form

$$k_T = C_z C_\alpha Eb [A'n^2 + B'],$$

or in the term of dimensionless groups as

$$\frac{k_T}{Eb} = C_z C_\alpha [A'n^2 + B'] \quad (10),$$

where  $C_z$  is the number of teeth correction,  $C_\alpha$  is the pressure angle correction, and  $A'$  and  $B'$  are constants.

## 5.2. Constants in the empirical formula

To find the constants  $A'$  and  $B'$  in Eq. (10), tooth stiffness values of all gears having the same number of teeth and the same pressure angle were considered. Here, the gear having 30 teeth with pressure angle of  $20^\circ$  was chosen as the reference. The FEM results of all gears having 30 teeth with pressure angle of  $20^\circ$  (Gear A-D) are shown in Fig. 5(d). The stiffness curves of all results almost completely identical. Here, the result of gear A that was calculated at the highest loading condition among all gears comparing with their maximum loading capacity was chosen to find the constants in Eq. (10), since its stiffness was convinced to be calculated from the linear elastic region.

Figure 8 shows the stiffness of the tooth pair of gear A. The vertical axis in this figure is  $k_T/(Eb)$ , and the

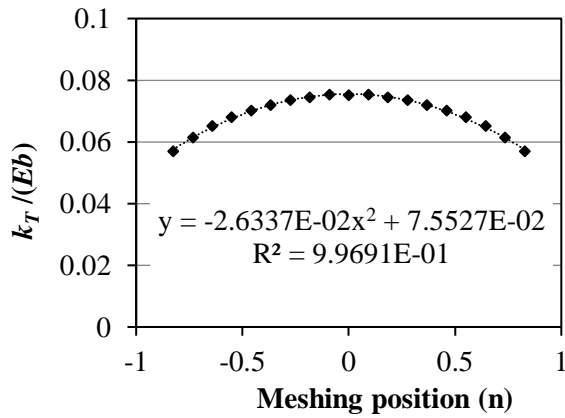


Fig. 8. Stiffness of the tooth pair of gear A.

horizontal axis is the meshing position,  $n$ . In this step, the correction  $C_z$  has not been considered. The pressure angle correction  $C_\alpha$  was set to be 1 in this case, since a pressure angle of  $20^\circ$  was selected to be the reference. From the figure, the data were arranged to form a convex curve. Using the polynomial regression method, the representative quadratic equation can be shown by

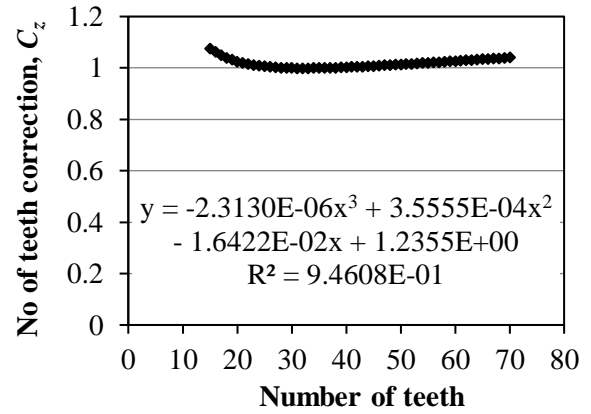
$$\left(\frac{k_T}{Eb}\right)_{\text{REF}} = (-2.6337 \times 10^{-2}) \cdot n^2 + 7.5527 \times 10^{-2} \quad (11).$$

Equation (11) represents the basic formula used to calculate tooth meshing stiffness. However, the accuracy of this formula can be increased by adding the number of teeth correction,  $C_z$  and the pressure angle correction,  $C_\alpha$ . The method to calculate these corrections will be described in the next section. By substituting the basic formula in Eq. (11) into Eq. (10), the empirical formula used to calculate gear tooth meshing stiffness can be written as

$$\frac{k_T}{Eb} = C_z C_\alpha [(-2.6337 \times 10^{-2}) \cdot n^2 + 7.5527 \times 10^{-2}] \quad (12).$$

### 5.3. Number of Teeth Correction

The effect of the number of teeth on the amount of tooth stiffness had been expressed in the formulae used to calculate the bending and contact torsional stiffness of the teeth in the Ref. [15] and the single stiffness in the Ref. [27]. Here, the formulae in the Ref. [15] were used to determine the tooth stiffness for the gear pair having 1:1 ratio with various teeth numbers. The correction  $C_z$  is defined as the ratio of the tooth stiffness and the tooth stiffness of the gear pair having 30 teeth. Figure 10 shows the values of the correction  $C_z$  at various teeth numbers  $z$ . The relation between these two parameters can be calculated by the polynomial regression method and shown by the equation

Fig. 9. Number of teeth correction  $C_z$ .

$$C_z = (-2.3130 \times 10^{-6})z^3 + (3.5555 \times 10^{-4})z^2 + (-1.6422 \times 10^{-2})z + 1.2355 \quad (13).$$

### 5.4. Pressure Angle Correction

The method used to calculate the pressure angle correction begins by plotting the values of  $k_T/(Eb)$  at various meshing positions as same as Fig 8. From Fig. 7(d), the stiffness curves of the gear pairs having the same pressure angle almost identical. Here, the gear pair G and H that have module 2 mm were used as the representative of the gear pair having a pressure angle  $14.5^\circ$  and  $25^\circ$ , respectively. Quadratic equations representing the values of  $k_T/(Eb)$  and the meshing position  $n$  can be written as:

$$\left(\frac{k_T}{Eb}\right)_{\alpha=14.5^\circ} = -1.5717 \times 10^{-2} \cdot n^2 + 5.7305 \times 10^{-2} \quad \text{for } \alpha = 14.5^\circ \quad (14),$$

and

$$\left(\frac{k_T}{Eb}\right)_{\alpha=25^\circ} = -6.5036 \times 10^{-2} \cdot n^2 + 8.8033 \times 10^{-2} \quad \text{for } \alpha = 25^\circ \quad (15).$$

Curve shapes of pressure angle  $14.5^\circ$  and  $25^\circ$  obviously differ from the curve of pressure angle  $20^\circ$  as shown in Fig. 7(d), indicating that the pressure angle correction should be a function of the meshing position  $n$ . The pressure angle correction  $C_\alpha$  at meshing position  $n$  is defined as the ratio between  $k_T/(Eb)$  of the pressure angle  $14.5^\circ$  or  $25^\circ$  calculated from Eqs.(14) or (15) and  $\left[k_T/(Eb)\right]_{\text{REF}}$  calculated from Eq. (11), and can be written as

$$C_\alpha = \left[ \left(\frac{k_T}{Eb}\right) / \left(\frac{k_T}{Eb}\right)_{\text{REF}} \right]_n \quad (16).$$

The values of  $C_\alpha$  calculated from Eq. (16) for pressure angles of  $14.5^\circ$  and  $25^\circ$  were plotted in Fig. 10.

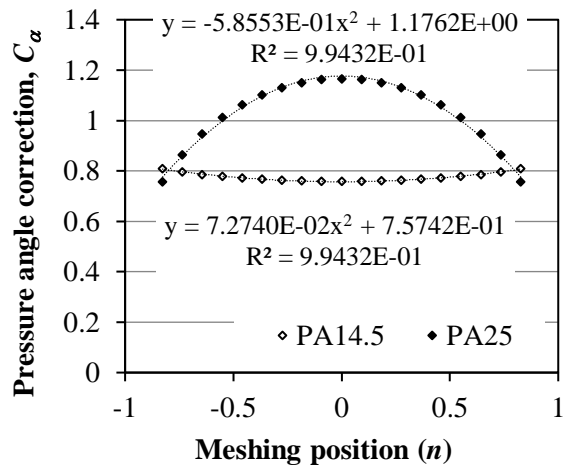


Fig. 10. Pressure angle correction  $C_\alpha$  at various meshing positions.

From these graphs, the equations used to calculate the pressure angle correction for pressure angles  $14.5^\circ$  and  $25^\circ$  can be determined by the polynomial regression method and are shown by equations

$$C_\alpha = 7.2740 \times 10^{-2} \cdot n^2 + 7.5742 \times 10^{-1} \quad \text{for } \alpha = 14.5^\circ \quad (17),$$

and

$$C_\alpha = -5.8553 \times 10^{-1} \cdot n^2 + 1.1762 \quad \text{for } \alpha = 25^\circ \quad (18).$$

## 6. Summary of The Procedure to Calculate Meshing Stiffness of a Gear Pair

The procedure to calculate the meshing stiffness of a spur gear pair can be summarized by the diagram in Fig. 11. First, the gear parameters as number of teeth, module, pressure angle, face width, root diameter and radius of shaft hole and material parameters as modulus of elasticity, shear modulus and Poisson's ratio must be known. The next step is to calculate the stiffness of the cylindrical body,  $k_C$  of both driving and driven side by Eq. (5).

Then the stiffness of the tooth pair is calculated by the empirical formula. There are four steps to calculate the stiffness of the tooth pair. The meshing position,  $n$  is calculated first, next the number of teeth corrections and the pressure angle correction are computed. When all parameters are known, the gear tooth stiffness can be determined by Eq. (12). By connecting the stiffness values of the cylindrical bodies of driving and driven side and the tooth stiffness, the stiffness of the spur gear pair can be obtained.

## 7. Verification of The Empirical Formula

The empirical formula was validated by calculating the meshing stiffness of the gear pairs and comparing the results with previous research of Hui Ma [6] and A. Fernandez del Rincon [22]. The stiffness was also

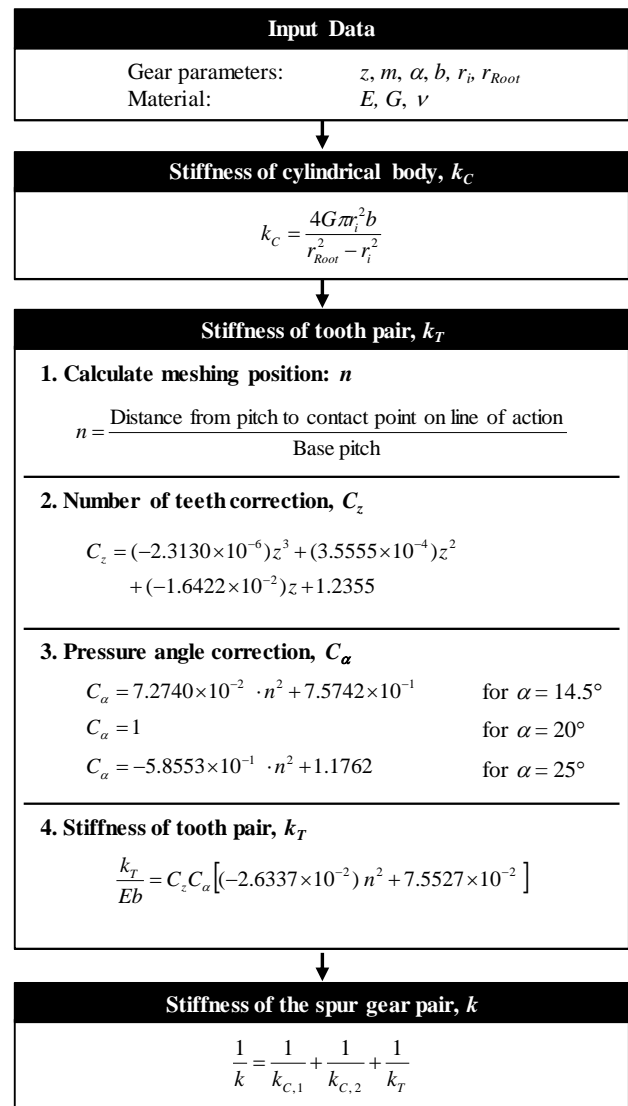


Fig. 11. Diagram of calculation procedure.

compared with the stiffness determined by the method in ISO 6336-1 [27].

## 7.1. Comparison with Hui Ma's Research

Hui Ma presented an analytical method to calculate meshing stiffness by the potential energy principle and the results were validated with the FEM results. The parameters of gear pairs in Hui Ma's research used for comparison are shown in Table 3, with calculation results shown in Fig. 12. Hui Ma calculated the results for two analytical methods as the traditional method (TM) in which the gear tooth was modelled as a cantilever beam on a base circle, and an improved method (IM) in which the gear tooth was considered as a cantilever beam on the root circle. The stiffness determined by the method in ISO 6336-1 was also plotted in this figure.

The stiffness calculated from the empirical formula fitted well with the results from the IM and FEM for both gear pairs. The stiffness estimated from the formula was slightly larger than the IM and FEM results in the single tooth contact zone. The parabolic shapes of the stiffness

Table 3. Parameters of the spur gear pairs used in Hui Ma's research

Parameter		Gear pair 1		Gear pair 2	
		Pinion	Gear	Pinion	Gear
Number of teeth		22	22	62	62
Young's modulus	GPa	206	206	206	206
Poisson's ratio		0.3	0.3	0.3	0.3
Module	mm	3	3	3	3
Tooth width	mm	20	20	20	20
Pressure angle	deg	20	20	20	20
Hub bore radius	mm	11.7	11.7	35.7	35.7

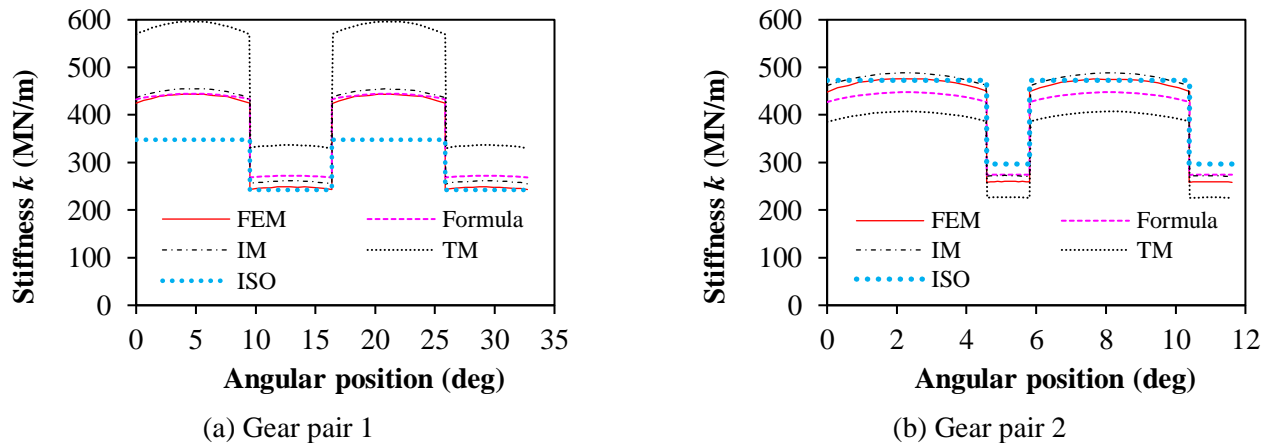


Fig. 12. Meshing stiffness of the gear pairs in Hui Ma's research.

from the empirical formula were similar to the Hui Ma's results. The maximum errors compared with FEM in both cases were around 10% and 6%, respectively. The RMS percentage errors of all positions were less than 7%. Results from the empirical formula were better than results from the TM in both cases.

Comparing with the stiffness from ISO 6336-1, although the stiffness from ISO 6336-1 were close to the FEM results in the single tooth contact zone of the gear pair 1 and in the double teeth contact zone of the gear pair 2, the large error occurred in the other zones. The maximum errors were around 20% and 14% for the gear pair 1 and the gear pair 2 respectively.

## 7.2. Comparison with Fernandez del Rincon's Research

Fernandez del Rincon et al proposed a model for calculating meshing stiffness based on a combination of the finite element model and an analytical approach derived from Hertzian contact theory. The parameters of the gear pair in this research are shown in Table 4. Although the results reported in this paper show that the gear meshing stiffness varied with load, at high load the meshing stiffness was almost constant, hence the result in the case of transmitted torque at 100 Nm as the largest load was picked for comparison. Stiffness values calculated using the methods proposed by Kuang's model and Cai's model and compared in Fernandez's paper and

the stiffness calculated by ISO 6336-1 method were also used here to compare with the result of the empirical formula.

Comparison of the meshing stiffness calculated by the empirical formula and results reported by Fernandez are shown in Fig. 13. Stiffness values calculated by the Fernandez model in this figure refer to the case when the deformation due to contacts on the adjacent teeth pairs were neglected. The stiffness calculated by the empirical formula agreed well with the results from the Fernandez model and Kuang's model in both single tooth contact zone and double teeth contact zone. The parabolic shape of the stiffness from the empirical formula was more similar to results calculated by Fernandez than results

Table 4. Parameters of the spur gear pair used in Fernandez's research.

Parameter	Value
Number of teeth	28
Gear ratio	1:1
Module	mm
Pressure angle	Deg
Face width	mm
Shaft radius	mm
Modulus of elasticity	GPa
Poisson's ratio	0.3

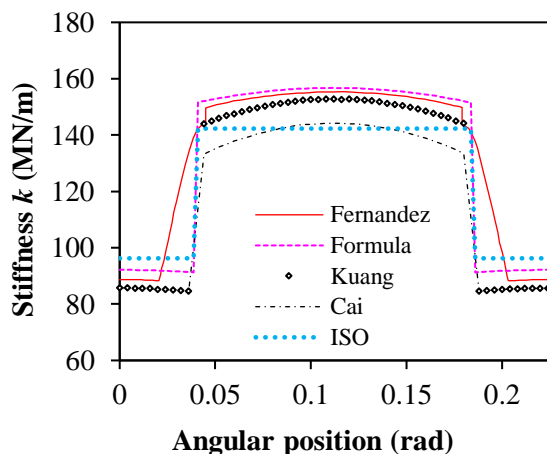


Fig. 13. Meshing stiffness of the gear pair in Fernandez's research.

from the Kuang and Cai models. The stiffness calculated from the empirical formula was much closer to the Fernandez's results than the stiffness calculated from the ISO 6336-1 in both single and double teeth contact zone.

## 8. Conclusions

Results confirmed that the empirical formula proposed here can be practically used to calculate gear meshing stiffness of the gear pair with gear ratio 1:1. The calculation is simple compared with other previously proposed analytical methods. The accuracy of our proposed empirical formula is high compared with the other analytical methods and the FEM. Maximum errors in most cases shown here were around 10%. The method to calculate the stiffness of the cylindrical body separately also makes the method proposed here can be applied to any gear pair having various cylindrical shapes and shaft radius. In contrast, the effect of shaft radius was not included in ISO 6336-1 calculation, hence the stiffness calculated from ISO 6336-1 will be constant for all solid disc gears having the same number of teeth. This will lead to the large amount of error when using the method in ISO 6336-1 in some cases.

Since this method is based on the curve fitting of the FEM results, the accuracy of the formula was significantly affected by the database results. Increasing the stiffness database and investigating the effect of other parameters that have not covered in this paper are suggested to further improve the accuracy of the empirical formula. Some of them are the application in the case of various gear ratios and the application at low load conditions. More data about the effect of number of teeth, pressure angle, and gear modifications should also be increased to improve the empirical formula.

Finally, it is worth mentioning that the use of FE solutions to construct an empirical formula using the method proposed in this paper can also be applied to other engineering applications where analytical methods or experiments are difficult to perform.

## Acknowledgement

This study was supported by the Department of Mechanical Engineering, Chulalongkorn University.

## References

- [1] R. W. Cornell, "Compliance and stress sensitivity of spur gear teeth," *J. Mech. Des. - T ASME*, vol. 103, no. 2, pp. 447-459, 1981.
- [2] T. H. Costopoulos and M. Spyropoulou "Tooth compliance and load distribution of spur gears," *Modelling, Measurement & Control*, vol. 54, no. 4, pp. 23-30, 1994.
- [3] I. Yesilyurt, F. Gu, and A. D. Ball, "Gear tooth stiffness reduction measurement using modal analysis and its use in wear fault severity assessment of spur gears," *NDT & E International*, vol. 36, no. 5, pp. 357-372, 2003.
- [4] F. Chaari, T. Fakhfakh, and M. Haddar, "Analytical modelling of spur gear tooth crack and influence on gearmesh stiffness," *European Journal of Mechanics A/Solids*, vol. 28, no. 3, pp. 461-468, 2009.
- [5] Z. Chen and Y. Shao, "Mesh stiffness calculation of a spur gear pair with tooth profile modification and tooth root crack," *Mechanism and Machine Theory*, vol. 62, pp. 63-74, 2013.
- [6] H. Ma, R. Song, X. Pang, B. Wen, "Time varying mesh stiffness calculation of cracked spur gears," *Engineering Failure Analysis*, vol. 44, pp. 179-194, 2014.
- [7] L. Cui, H. Zhai, and F. Zhang, "Research on the meshing stiffness and vibration response of cracked gears based on the universal equation of gear profile," *Mechanism and Machine Theory*, vol. 94, pp. 80-95, 2015.
- [8] A. Saxena, A. Parey, and M. Chouksey, "Effect of shaft misalignment and friction force on time varying mesh stiffness of spur gear pair," *Engineering Failure Analysis*, vol. 49, pp. 79-91, 2015.
- [9] Z. Chen, W. Zhai, Y. Shao, K. Wang, and G. Sun, "Analytical model for mesh stiffness calculation of spur gear pair with non-uniformly distributed tooth root crack," *Engineering Failure Analysis*, vol. 66, pp. 502-514, 2016.
- [10] A. Saxena, A. Parey, and M. Chouksey, "Time varying mesh stiffness calculation of spur gear pair considering sliding friction and spalling defects," *Engineering Failure Analysis*, vol. 70, pp. 200-211, 2016.
- [11] Y. Lei, D. Wang, Z. Liu, and X. Yang, "A new model for calculating time-varying gearmesh stiffness," *Vibroengineering Procedia*, vol. 14, pp. 334-339, 2017.
- [12] M. B. Sánchez, M. Pleguezuelos, and J. I. Pedrero, "Approximate equations for the meshing stiffness and the load sharing ratio of spur gears including Hertzian effects," *Mechanism and Machine Theory*, vol. 109, pp. 231-249, 2017.
- [13] M. H. Arafa and M. M. Megahed, "Evaluation of spur gear mesh compliance using the finite element method," *Proceedings of the Institution of Mechanical*

- Engineers, Part C: Journal of Mechanical Engineering Science*, vol. 213, no. 6, pp. 569-579, 1999.
- [14] J. D. Wang and I. M. Howard, "Error analysis on finite element modeling of involute spur gears," *J. Mech. Des. – T ASME*, vol. 128, no. 1, pp. 90-97, 2006.
- [15] T. Kiekbusch, D. Sappok, B. Sauer, and I. Howard, "Calculation of the combined torsional mesh stiffness of spur gears with two- and three-dimensional parametrical FE models," *Journal of Mechanical Engineering*, vol. 57, no. 11, pp. 810-818, 2011.
- [16] N. L. Pedersen and M. F. Jørgensen, "On gear tooth stiffness evaluation," *Computer and Structure*, vol. 135, pp. 109-117, 2014.
- [17] C. G. Cooley, C. Liu, X. Dai, and R. G. Parker, "Gear tooth mesh stiffness: A comparison of calculation approaches," *Mechanism and Machine Theory*, vol. 105, pp. 540-553, 2016.
- [18] F. Karpat, O. Doğan, C. Yuce, and S. Ekwaro-Osire, "An improved numerical method for the mesh stiffness calculation of spur gears with asymmetric teeth on dynamic load analysis," *Advances in Mechanical Engineering*, vol. 9, no. 8, pp. 1-12, 2017.
- [19] X. Liang, H. Zhang, M. J. Zuo, and Y. Qin, "Three new models for evaluation of standard involute spur gear mesh stiffness," *Mechanical Systems and Signal Processing*, vol. 101, pp. 424-434, 2018.
- [20] R. G. Munro, D. Palmer, and L. Morrish, "An experimental method to measure gear tooth stiffness throughout and beyond the path of contact," *Proceedings of the Institution of Mechanical Engineers, Part C: Journal of Mechanical Engineering Science*, vol. 215, no. 7, pp. 793-803, 2001.
- [21] F. Karpat, C. Yuce, and O. Doğan, "Experimental measurement and numerical validation of single tooth stiffness for involute spur gears," *Measurement*, vol. 150, p. 107043, 2020.
- [22] A. Fernandez del Rincon, F. Viadero, M. Iglesias, P. Garcia, A. de-Juan, and R. Sancibrian, "A model for the study of meshing stiffness in spur gear transmissions," *Mechanism and Machine Theory*, vol. 61, pp. 30-58, 2013.
- [23] H. Ma, X. Pang, R. Feng, J. Zeng, and B. Wen, "Improved time-varying mesh stiffness model of cracked spur gears," *Engineering Failure Analysis*, vol. 55, pp. 271-287, 2015.
- [24] H. Ma, J. Zeng, R. Feng, X. Pang, and B. Wen, "An improved analytical method for mesh stiffness calculation of spur gears with tip relief," *Mechanical and Machine Theory*, vol. 98, pp. 64-80, 2016.
- [25] S. Feng, L. Chang, and Z. He, "A hybrid finite element and analytical model for determining the mesh stiffness of internal gear pairs," *Journal of Mechanical Science and Technology*, vol. 34, no. 6, pp. 2477-2485, 2020.
- [26] S. Timoshenko and J. N. Goodier, "Two-dimensional problems in polar coordinates," in *Theory of Elasticity*. McGraw-Hill Book Company, Inc., 1951, ch. 4, pp. 107-111.
- [27] *Calculation of Load Capacity of Spur and Helical Gears – Part I: Basic Principles, Introduction and Influence Factors*, International Standard ISO 6336-1:2006, 2006, pp. 70-75.



**Thiwa Nantapak** received the B.Eng. in Mechanical Engineering from Khon Kaen University in 2016, M.Eng. in Mechanical Engineering from Chulalongkorn University in 2019 respectively. He is presently a graduate research assistant in faculty of engineering, Chulalongkorn University. His research includes design engineering, R&D engineering in the field of Medical Devices.



**Korn Sara Srisarakorn** received a bachelor's degree in mechanical engineering from Chulalongkorn University in 2019. She is presently a design engineer at Hino motors manufacturing (Thailand) Ltd. Her responsibilities included truck and bus frame design.



**Thanakorn Tantipiriyapongs** received his bachelor's degree in mechanical engineering from Chulalongkorn University in 2019. He is presently studying in Master of Engineering Program in Automotive and Advanced Transportation Engineering, King Mongkut's Institute of Technology Ladkrabang. He is doing a research in the field of automotive engineering.



**Nitchawat Deecharoen** received a bachelor's degree in mechanical engineering from Chulalongkorn University in 2019. He is presently a design engineer at YIC Asia-Pacific Corporation Co., Ltd. His responsibilities included automotive wire harness protective parts design



**Chanat Ratanasumawong** was born in Bangkok, Thailand in 1977. He received the B.S. and M.S. degrees in mechanical engineering from Chulalongkorn University, Thailand, in 1998 and in 2001 respectively. He completed his doctoral degree in precision machinery systems from Tokyo Institute of Technology, Japan, in 2006. He is currently an associate professor in the department of mechanical engineering, Chulalongkorn University. Dr. Chanat's research interests focus on the gear vibration, gear efficiency, machine vibration and machine design.